Earth and Planetary Science Letters 283 (2009) 174–180

Contents lists available at ScienceDirect

Earth and Planetary Science Letters

journal homepage: www.elsevier.com/locate/epsl

Compositional dependence of structural transition pressures in amorphous phases with mantle-related compositions

Sang-Heon Shim *, Krystle Catalli

Department of Earth, Atmospheric, and Planetary Sciences, Massachusetts Institute of Technology, United States

ARTICLE INFO

Article history:
Received 5 December 2008
Received in revised form 24 March 2009
Accepted 14 April 2009
Available online 13 May 2009

Editor: L. Stixrude

Keywords:
silicate glasses
structural transition
compositional sensitivity
Raman spectroscopy
mantle differentiation

ABSTRACT

Properties of silicate melts are key to understanding the evolution of the mantles of the Earth and terrestrial planets. Although remarkable progress has been made in first-principle calculations for melts in recent years, structural measurements of silicate melts at in situ high *P–T* remain one of the most challenging tasks. The study of glasses, kinetically frozen melts, at high pressure can provide valuable insights into related melts in the mantle. We report Raman scattering of $MgSiO_3$ glass revealing a structural transition at 19–38 GPa, which is associated with increases in the Si – O coordination number, and another transition at 65–70 GPa. However, in $CaSiO_3$ and Mg_2SiO_4 glasses, the former transition occurs at higher pressures by 5–10 GPa and the latter transition is not observed to our maximum pressure (80 GPa), indicating that a less polymerized Si – O network increases the transition pressures. Our results suggest that the pressure for the structural transitions in these glasses is influenced strongly by the concentration of network former cations and the ionic size of the network modifiers. This observation may have important implications for compositional differentiation in the early magma ocean and the present-day mantle.

1. Introduction

Giant impacts, such as the Moon forming event, are sufficiently energetic to result in a magma ocean extending into the deep mantle (Tonks and Melosh, 1993). The processes in the magma ocean determine the initial conditions for the composition and structure of the mantle (Ohtani et al., 1986; Ito and Takahashi, 1987; Agee and Walker, 1988; Agee, 1990; Miller et al., 1991; Boyet and Carlson, 2005). In the present-day mantle, seismic evidence suggests the existence of melts atop the transition zone (Revenaugh and Sipkin, 1994; Song et al., 2004) and the core–mantle boundary (CMB) (Revenaugh and Meyer, 1997; Williams et al., 1998).

Although remarkable progress has been made in first-principle calculations for melts in recent years (Stixrude and Karki, 2005; Wan et al., 2007; Mookherjee et al., 2008; de Koker et al., 2008), measurements of silicate melt structures at in situ high *P–T* remain challenging. For example, X-ray scattering provides information on the coordination state and bond lengths in amorphous phases. While the technique has been applied to low-*P* measurements or samples with large scattering cross sections (Shen et al., 2004), scattering from amorphous materials with mantle-related compositions in the diamond-anvil cell is difficult due to the large contribution from thick diamond anvils and weak scattering cross sections from important cations in the mantle, such as Mg and Si. Shockwave measurements provide constraints on the density of melts at in situ high *P–T* (Rigden et al., 1984; Akins et al., 2004; Mosenfelder et al., 2007). However, it does not provide information on the structure of melt.

Vibrational spectroscopy can provide valuable information on amorphous phases (McMillan, 1984b). However, structural measurements within the stability field of melt at high pressure are rare and a pioneering attempt has been made only for a silicate melt analog (Farber and Williams, 1992).

Studies for alkali silicate glasses quenched from melts at high *P–T* have shown intriguing features formed at high pressures (Xue et al., 1989; Stebbins and McMillan, 1989; Xue et al., 1991; Lee et al., 2003). However, due to relaxation effects during decompression, some degree of uncertainty is unavoidable. In addition, these types of studies have been limited to shallow mantle pressures ($\lesssim$10 GPa). In situ studies of glasses, kinetically frozen melts, in the diamond-anvil cell can provide valuable insights on related melts to much higher pressures (Hemley et al., 1986; Williams and Jeanloz, 1988). Previous spectroscopic studies on silicate glasses have revealed decreases in the angles between the corner shared SiO_4 tetrahedra ($\angle$Si – O – Si) (Hemley et al., 1986) and increases in the Si – O coordination numbers (Williams and Jeanloz, 1988) at high pressure. These changes occur over a wide pressure range, which is in contrast with their crystalline counterparts. These structural changes are able to explain the rapid density increase of silicate melts at high pressure and support the prediction that the densities of silicate melts become similar to those of crystalline phases in the deep interior (Stolper and Ahrens, 1987), leading to neutrally or even negatively buoyant melts in the deep mantle (Rigden et al., 1984; Akins et al., 2004; Mosenfelder et al., 2007).

* Corresponding author.
E-mail address: sangshim@mit.edu (S.-H. Shim).

0012-821X/$ – see front matter © 2009 Elsevier B.V. All rights reserved.
doi:10.1016/j.epsl.2009.04.018

However, the compressional behavior of amorphous forms of major mantle components, such as $MgSiO_3$ and Mg_2SiO_4, has not been studied well at high pressure. Previous vibrational spectroscopy studies on them have failed to identify the changes found in other silicate glasses (Kubicki et al., 1992; Durben et al., 1993). The main reasons have been the difficulty in quenching melts with low silica contents and the extremely weak light scattering of Mg silicate glasses (McMillan, 1984a).

Recently, high-quality Mg silicate glasses have been synthesized using the containerless method (Tangeman et al., 2001). This development has facilitated exciting discoveries in Mg silicate glasses at ambient conditions. In Mg_2SiO_4, the low Si concentration forces Mg to participate in the glass network (Kohara et al., 2004). Studies on $MgSiO_3$–Mg_2SiO_4 revealed a strong sensitivity of the network structure to Si concentration at 1 bar (Wilding et al., 2004a,b). Here, we report Raman scattering of $MgSiO_3$, Mg_2SiO_4, and $CaSiO_3$ glasses, synthesized using the containerless method, at in situ high pressure up to 80 GPa in the diamond-anvil cell.

2. Experimental methods

We obtained $MgSiO_3$, Mg_2SiO_4, and $CaSiO_3$ glasses using the containerless synthesis method (Tangeman et al., 2001). In containerless synthesis, a stream of pure gas (such as oxygen or argon) levitates a crystalline beam made from a mixture of component oxides. While it is levitated, the sample is heated and melted by a continuous-wave CO_2 laser beam. Samples are quenched by blocking the laser beam. Therefore, contamination and heterogeneous nucleation in conventional methods can be prevented (Tangeman et al., 2001).

The homogeneity and purity of the glasses synthesized by this method have been confirmed in recent studies (Tangeman et al., 2001; Kohara et al., 2004; Wilding et al., 2004a,b). We also examined the chemical compositions of these glasses with Electron Microprobe at MIT. No evidence of crystalline inclusions has been found in our synchrotron X-ray diffraction, Raman scattering, and electron microscopy measurements except for Mg_2SiO_4 glass where about 1% of crystalline (likely olivine) inclusions were found. Previous NMR measurements also detected 1% of crystalline inclusions in Mg_2SiO_4 glass synthesized using the same method (Tangeman et al., 2001). For Mg_2SiO_4 glass, we inspected the sample using Raman spectroscopy and chose the areas that contain only the amorphous phase.

Each of the $MgSiO_3$, Mg_2SiO_4, and $CaSiO_3$ glasses was loaded in a preindented Re gasket in a diamond-anvil cell. At least three high-pressure runs were conducted for each glass. Ruby chips were loaded together with the samples for pressure measurements (Mao et al., 1986). We used synthetic diamonds with high optical quality for the anvils. An Ar/Kr mixed ion laser beam (514.5 nm) was focused to a 2-μm spot on the sample in the diamond cell. Raman scattering was measured for 40 min at each pressure point using a CCD detector. Wavenumber calibration of the spectrometer was conducted with a Ne lamp.

Mg silicate glasses have the weakest Raman scattering among alkali and alkaline earth silicate glasses (McMillan, 1984a), and Raman modes of glasses are broad due to structural disorder. Any uncorrected optical system responses, such as irregularities in CCD detector sensitivities, can introduce artifacts in the measured spectra if they are not corrected properly. Therefore, we measured optical system responses using NIST's Raman intensity standard (Choquette et al., 2007) and corrected all the spectra for the measured optical responses. Spectral fitting was conducted using a symmetric pseudo-voigt peak profile shape function.

We conducted Raman measurements with an Ar medium and without a medium. However, no noticeable difference was detected, including peak widths, except for a lower signal-to-background ratio in an Ar medium due to the smaller thickness of the sample in an Ar pressure medium. Therefore, we present only measurements collected without a medium as spectral features are better resolved at high pressure.

3. Results

Silicate glasses have two groups of Raman modes at ambient conditions (McMillan, 1984b): the Si–O–Si bending vibrations (b_1–b_3 in Fig. 1) between 400 and 750 cm^{-1} and the Si–O stretching vibrations between 800 and 1100 cm^{-1} (Q^n in Fig. 1). The frequencies of the stretching vibrations are related to the degree of polymerization of the SiO_4 tetrahedral network: the tetrahedra with zero (Q^0), one (Q^1), two (Q^2), and three (Q^3) bridging oxygens are associated with the modes at 850, 900, 950–1000, and 1050–1100 cm^{-1}, respectively (McMillan, 1984b).

Upon compression, the frequencies of both bending and stretching modes increase in $MgSiO_3$ glass (Figs. 2a and 3a). Between 14 and 20 GPa, the rate of frequency increase becomes much larger and the intensities of b_2, Q^2, and Q^3 rapidly decrease while the Q^1 intensity increases. Similar to other silicate glasses and melts (Rigden et al., 1984; Hemley et al., 1986), all these changes can be attributed to decreases in both the ∠Si–O–Si angles and the number of tetrahedra per ring and chain with pressure, which is also consistent with an NMR study of $MgSiO_3$ glass compressed to 10 GPa (Gaudio et al., 2008).

Starting at 20 GPa, a significant intensity growth was detected at a frequency between the bending and stretching modes (ν in Fig. 2a). The bending mode finally disappears at 28 GPa while the new mode continues to grow with pressure. The intensities of Q^2 and Q^3 continue to decrease, and the Q^1 frequency becomes much less sensitive to pressure above 30 GPa (Fig. 3a). Finally, at 37 GPa, the spectrum has only a single peak with a symmetric shape (ν' in Fig. 2a).

Although the frequency of ν' lies between Q^1 and ν, its pressure-induced shift is much closer to that of ν (Fig. 3a). There appears to be a discontinuous increase by 50 cm^{-1} between the frequencies of ν and ν'at 37 GPa in $MgSiO_3$ glass (at 45 GPa in $CaSiO_3$ glass, see below). The completion of the structural transitions may result in a change in the surrounding environments for the Si–O bonding, possibly leading to a discontinuity in the frequency of the Si–O stretching mode. On the other hand, this apparent offset could be an artifact as there exists considerable uncertainty in the frequency of the new mode (ν) due to severe peak overlap with the Q^0 or Q^1 mode below 40 GPa. Therefore, together with the peak shape, the behavior of ν' suggests completion of a structural change or at least dominance of the high-pressure structure above 37 GPa in $MgSiO_3$ glass.

The frequency of the new mode (ν and ν') is systematically lower by 50–100 cm^{-1} than that of Q^0 observed in $CaSiO_3$ and Mg_2SiO_4

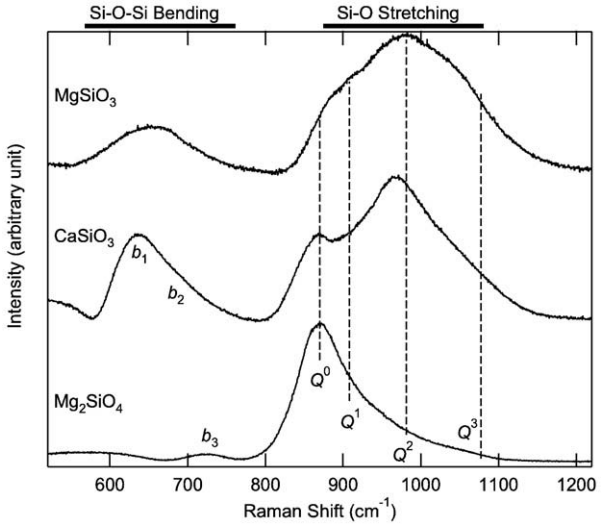

Fig. 1. Raman spectra of silicate glasses with different degrees of polymerization at ambient pressure. The Si–O stretching modes (Q^n) are labeled by the number of bridging oxygens. The Si–O–Si bending modes (b_n) are labeled in order of their frequencies. The vertical dashed lines are guides for the eye.

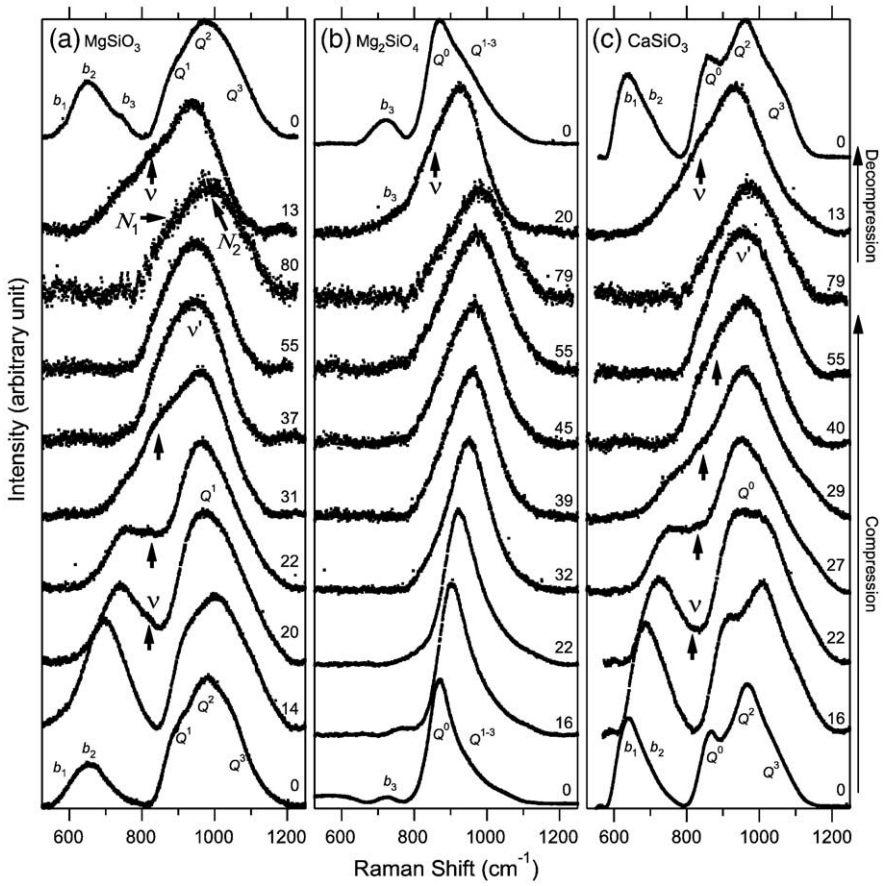

Fig. 2. Raman spectra of (a) $MgSiO_3$, (b) Mg_2SiO_4, and (c) $CaSiO_3$ glasses at high pressure. The values at the right side of the spectra are pressures (in GPa) where the spectra were measured. The Si – O – Si bending modes (b_1–b_3) and Si – O stretching modes (Q^0–Q^3) are labeled in order of their frequency and number of bridging oxygens, respectively. The new mode associated with the Si – O coordination number increase is labeled as ν (ν' after the completion of the structural transition). Two new modes observed above 65 GPa in $MgSiO_3$ glass are labeled as N_1 and N_2. The backgrounds were subtracted.

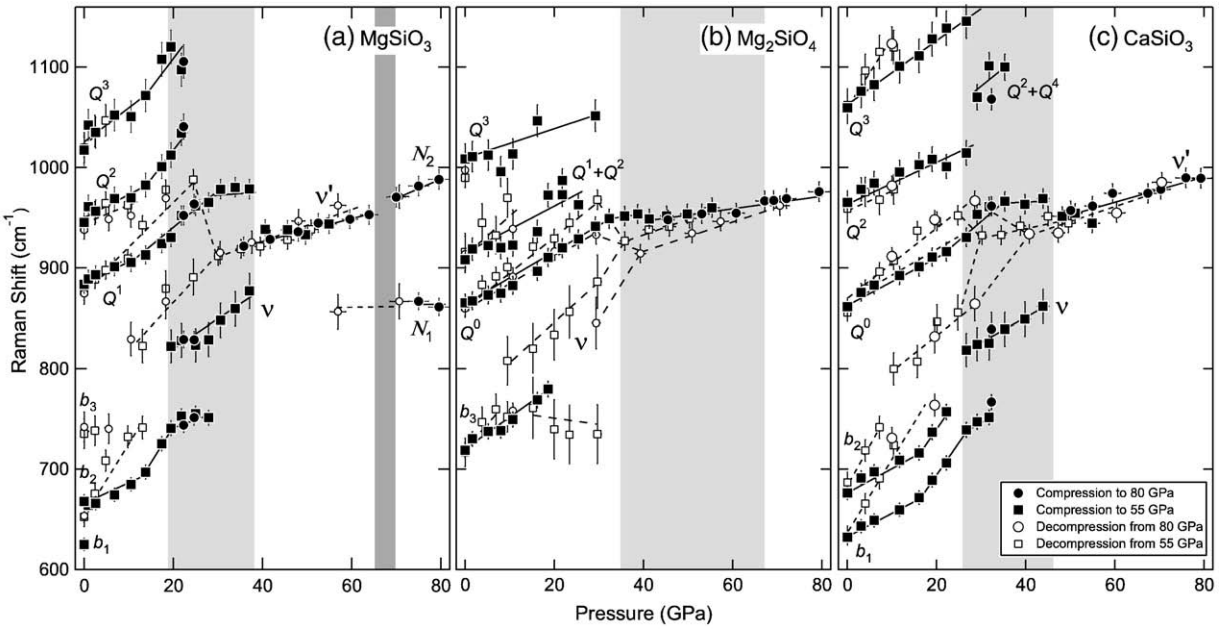

Fig. 3. Mode frequencies of (a) $MgSiO_3$, (b) Mg_2SiO_4, and (c) $CaSiO_3$ glasses at high pressure. The solid and open symbols are for the data points measured during compression and decompression, respectively. The circles and squares are for the data points from runs with maximum pressures of 55 and 80 GPa, respectively. The solid and dashed lines are guides for the eye for compression and decompression data points, respectively. The grey areas are the pressure range where both 4-fold and higher coordinated Si atoms coexist. The dark grey area is the pressure range where another spectral change was observed in $MgSiO_3$ glass. The labels are the same as those in Fig. 2.

glasses at high pressure (Fig. 3b,c). In fact, in $CaSiO_3$ glass, we found the appearance of ν while Q^0 still exists. Therefore, we rule out the possibility of transition from Q^1 to Q^0.

In crystalline phases, the Si–O stretching vibration in higher Si–O coordinations should have lower frequency than in tetrahedral coordination (Navrotsky, 1980). In the perovskite (Karki et al., 2000) and ilmenite (Wentzcovitch et al., 2004) phases in $MgSiO_3$, in which all Si atoms are in 6-fold coordination, the SiO_6 octahedral vibrations lie between 750 and 950 cm^{-1} and between 880 and 900 cm^{-1}, respectively, at 30 GPa. The Si–O stretching frequency in SiO_5 is unknown. However, it should still be lower than that of SiO_4. The frequency of the new mode (ν and ν') lies within this range and therefore is consistent with an increase in Si–O coordination number (to SiO_5 and SiO_6).

Different structural models have been suggested to explain the changes in glasses and melts at high pressures (Stolper and Ahrens, 1987; Wolf et al., 1990; Xue et al., 1991; Lee et al., 2008; de Koker et al., 2008). Stolper and Ahrens (1987) proposed that gradual decreases in the ∠Si–O–Si angles among the corner shared SiO_4 tetrahedra with pressure ultimately result in oxygen arrangements which can be described as polymerized SiO_6 octahedra in amorphous silicates. According to this prediction, high-coordinated Si will appear while the ∠Si–O–Si angles decrease, which is reflected in our observation of a rapid increase in the Si–O–Si bending frequency and a growth of the ν intensity while the intensities of the stretching and bending vibrations of the SiO_4 tetrahedra decrease (Figs. 2 and 3). Although the simple schematic model by Stolper and Ahrens (1987) does not predict the formation of SiO_5, recent computer simulations (de Koker et al., 2008) have shown that the Si–O coordination number increases gradually (4→5→6) with pressure in Mg-silicate melts. Therefore, our Raman observations can be interpreted that decreases in the size of the SiO_4 tetrahedral chains or rings and consumption of the polymerized SiO_4 occur to increase the population of high-coordinated Si, such as SiO_5 and SiO_6.

The lower rate of increase in the Q^1 frequency above 30 GPa where ν rapidly grows suggests that the density increase of $MgSiO_3$ glass at this pressure range is achieved mainly by increasing the Si–O coordination number, not by the compaction of the SiO_4 network. In addition, Q^1 survives to higher pressure than any other stretching modes, suggesting that the depolymerized tetrahedra are much more difficult to transform to higher coordinations than the polymerized SiO_4 tetrahedra, also consistent with the model of Stolper and Ahrens (1987).

Above 65 GPa, $MgSiO_3$ glass shows another spectral change (Fig. 2a). The ν' mode becomes much broader and asymmetric, indicating peak splitting into at least two modes (N_1 and N_2 in Fig. 3a). In $MgSiO_3$ crystalline phases, edge sharing among the SiO_6 octahedra appears during the phase transition from perovskite to postperovskite (Murakami et al., 2004; Shim et al., 2008). In Raman measurements of $MgGeO_3$, modes tend to shift to higher frequencies during the phase transition from perovskite to postperovskite (Shim et al., 2007). Our Raman spectroscopy on $MgSiO_3$ glass reveals a slight increase in frequency at 65 GPa (N_2 in Fig. 3a), and therefore we tentatively assign this to the connectivity changes among SiO_5 and SiO_6. The appearance of a low-frequency mode (N_1) could be related to the Si–O–Si bending vibration in the high-coordinated Si–O network. However, more constraints are necessary for the structural assignments of this spectral change.

In the Raman spectrum of Mg_2SiO_4 glass, the most pronounced difference is the dominance of Q^0, i.e., the isolated SiO_4 tetrahedra, consistent with recent X-ray studies (Kohara et al., 2004; Wilding et al., 2004b) and previous Raman studies (Piriou and McMillan, 1983; Williams et al., 1989; Cooney and Sharma, 1990) at ambient pressure (Fig. 2b). The bending mode shows an increase in frequency with pressure and finally disappears into Q^0 at 20 GPa (Fig. 2b). In addition, the Q^{1-3} intensity decreases with pressure, suggesting a decrease in the population of polymerized SiO_4 tetrahedra. However, no clear evidence of the new mode was found in Mg_2SiO_4 glass during compression up to 80 GPa, which is in sharp contrast with the case of $MgSiO_3$ glass. As observed in $MgSiO_3$ glass, this may be due to the difficulty in transforming the isolated SiO_4 tetrahedra into the SiO_6 octahedra.

Our measurements of Mg_2SiO_4 glass before compression reveal that it contains a small amount of polymerized SiO_4 tetrahedra, consistent with recent X-ray studies (Kohara et al., 2004; Wilding et al., 2004b) (Fig. 1). Therefore, some amount of Si atoms may be in higher coordinations at high pressure even in Mg_2SiO_4 glass. This hypothesis can be supported by the following observations.

Although it is not clear during compression, ν is observed during decompression at $10 \le P \le 20$ GPa through an asymmetric shape of the dominant singlet in Mg_2SiO_4 glass (Fig. 2b). The frequency agrees with that observed for ν in $MgSiO_3$ glass (Fig. 3b). In addition, there are

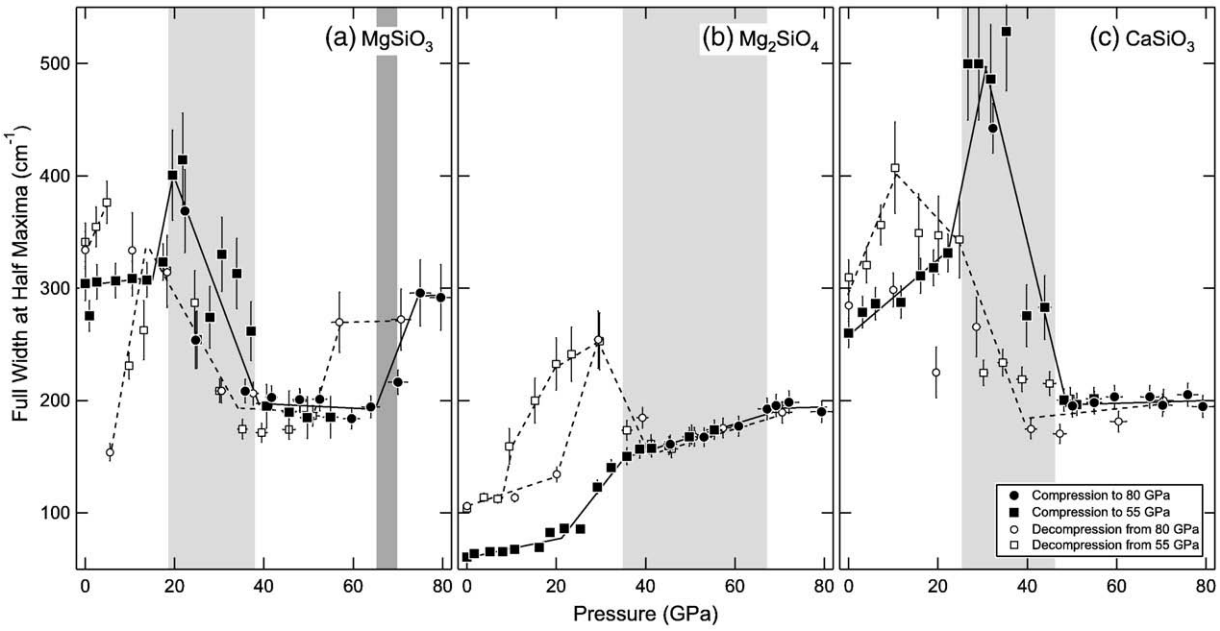

Fig. 4. Full width at half maxima (FWHM) of the Si–O stretching vibrations in (a) $MgSiO_3$, (b) Mg_2SiO_4, and (c) $CaSiO_3$ glasses at high pressure. The width is calculated from the sum of all the modes existing in the Si–O stretching frequency range (Q^0–Q^3, ν, ν', N_1, and N_2). The notations are the same as those in Fig. 3.

lines of evidence that ν may already exist during compression in Mg_2SiO_4 glass. For example, the Q^0 frequency becomes much less sensitive to pressure at $P \geq 32$ GPa, which was also seen in a previous Raman study (Durben et al., 1993), similar to what was found in $MgSiO_3$ glass during the appearance of the new mode. However, the rate of the pressure-induced shift of the dominant singlet at $P \geq 32$ GPa remains much smaller in Mg_2SiO_4 glass compared with $MgSiO_3$ glass (ν'), suggesting that the dominant singlet in Mg_2SiO_4 glass at $P \geq 32$ GPa may be a combination of the low-intensity stretching mode (ν) of SiO_5 and SiO_6, and the high-intensity Q^0 mode of SiO_4. The reason that ν was observed more clearly during decompression is perhaps because the frequency of ν becomes sufficiently distinct from that of Q^0 at lower pressure.

During decompression, the frequency of the singlet follows different trajectories depending on the maximum pressure in Mg_2SiO_4 (Fig. 3b) unlike in $MgSiO_3$ glass. This suggests that the structure of Mg_2SiO_4 glass at 55 GPa is different from that at 80 GPa. In other words, if the population of the high-coordinated Si is smaller in the sample compressed to 55 GPa, the surrounding glass network for the SiO_5 or SiO_6 species would be different from that at 80 GPa, leading to a different frequency during decompression.

Finally, although most high-pressure features are lost during decompression, the Q^{1-3} intensity increases after pressure quench in Mg_2SiO_4 glass (Fig. 2b). It can be postulated from the model of Stolper and Ahrens (1987) that SiO_6 (and SiO_5) would break into polymerized SiO_4 tetrahedra during decompression. Therefore, the enhanced Q^{1-3} intensity after decompression may be because of incomplete relaxation of the high-pressure structure.

An important observation is that the features related to the structural transition appeared at systematically higher pressure by at least 15 GPa in Mg_2SiO_4 glass compared with $MgSiO_3$ glass. Moreover, whereas the structural transition appears to be completed by 37 GPa in $MgSiO_3$ glass, in Mg_2SiO_4 glass the transition is not completed until at least 65 GPa where we found a slightly different trend in width (Fig. 4).

The ambient pressure spectrum of $CaSiO_3$ glass shows spectral features intermediate between $MgSiO_3$ and Mg_2SiO_4 glasses. We assign the lowest frequency stretching mode to Q^0 as its frequency matches with that of the Q^2 mode in Mg_2SiO_4 for which X-ray scattering studies have shown a dominant population of the isolated tetrahedra (Kohara et al., 2004; Wilding et al., 2004b) (Fig. 1). Therefore, we believe that $CaSiO_3$ glass has isolated tetrahedra (Q^0) as well as polymerized tetrahedra (Q^1–Q^3) (Fig. 2). Because Ca is much larger in size than Mg, it may break some tetrahedral rings, leading to an increased Q^0 population.

The high-pressure behaviors of $CaSiO_3$ glass are similar to $MgSiO_3$ glass, including the appearance of the new mode (ν). However, the spectral changes were observed at systematically higher pressure (by 5–10 GPa). For example, Q^0 still survives at 44 GPa in $CaSiO_3$ glass (Figs. 2 and 3) whereas $MgSiO_3$ glass appears to transform completely by 37 GPa. Combined with the observations for Mg_2SiO_4 glass, the high-pressure behaviors of $CaSiO_3$ glass indicate that the isolated SiO_4 tetrahedra (Q^0) remain untransformed to high pressure, delaying the completion of the structural transition in $CaSiO_3$ and Mg_2SiO_4 glasses.

Although most of the new spectral features at high pressure disappear during decompression, the spectra of $CaSiO_3$ glass after pressure quench reveal relative increases in the intensities of Q^0 and Q^3. Similar to Mg_2SiO_4 glass, the increased Q^3 intensity is likely due to the formation of a more polymerized network by the break up of SiO_5 or SiO_6 during decompression. An increase in the Q^0 intensity was also observed in the sample quenched from 25 GPa which is lower than the transition pressure. Therefore, this should be related to lower pressure processes. Perhaps the large size of the Ca^{2+} ion prohibits the tetrahedral rings from decreasing below a certain limit, leaving broken rings, and increasing the number of non-bridging oxygens during decompression from 25 GPa.

In $CaSiO_3$ and Mg_2SiO_4 glasses, no evidence for the transition observed in $MgSiO_3$ glass at 65 GPa was found to 80 GPa. We also attribute this difference to the dominantly (Mg_2SiO_4) or partially ($CaSiO_3$) depolymerized network in these glasses.

Further evidence of the more gradual transition in Mg_2SiO_4 glass can be found in the peak width (Fig. 4). The total width of the modes existing in the Si – O stretching vibration frequency range (such as Q^0–Q^3, ν, ν', N_1, and N_2) provides insights into the diversity in the coordination and polymerization of the Si – O polyhedra. During the structural transition, the total width is larger due to the coexistence of both low-pressure and high-pressure configurations in the glass structures. Relatively large uncertainty (2σ) in the total width is due to severe peak overlaps among the modes. $MgSiO_3$ and $CaSiO_3$ glasses show similar behaviors with pressure (Fig. 4), but with systematically higher pressure in $CaSiO_3$ glass consistent with the trend observed in frequency (Fig. 3). However, Mg_2SiO_4 glass shows very different behaviors from these two glasses, indicating a distinct structural state of this glass from the other two glasses at high pressure.

The peak width is expected to increase with compression due to deviatoric stress as well. However, the abrupt changes at 17 and 31 GPa cannot be explained by a gradual increase in peak width expected for deviatoric stress. In addition, our measurements with an argon pressure medium show no significant differences in the width.

4. Discussion

Our Raman spectroscopy shows that the dominant compressional mechanisms in Mg-silicate glasses are: decreases in the ∠Si – O – Si angles and in the numbers of the SiO_4 tetrahedra in rings or chains of the framework at lower pressure, and increases in the Si – O coordination number at higher pressure. More importantly, the transition pressures are sensitive to the degree of polymerization of the Si – O network, leading to higher transition pressures in glasses with low Si concentration and large network modifier cations.

Interestingly, this compositional dependence of the transition pressure for the appearance of high-coordinated Si can be found in crystalline phases in the same compositional systems as well. In Mg_2SiO_4, all Si atoms remain 4-fold coordinated until the system breaks down into $MgSiO_3$-perovskite + MgO-periclase at a depth of 660 km in the mantle. However, in $MgSiO_3$, the SiO_6 octahedra appear from shallower depths, 500–600 km, in the garnet and ilmenite phases.

There exist some limitations in the extrapolation of the structural behaviors of metastable glasses measured at high-P and room-T to the behaviors of melts stable at high P–T. For example, some structural differences have been documented between glasses at high P and room T and glasses quenched from melts at high P and high T in some systems (Mackenzie, 1963a,b; McMillan et al., 1984; Yarger et al., 1995; Wolf and McMillan, 1995).

Computational simulations (Stixrude and Karki, 2005; de Koker et al., 2008) showed that the dynamic nature of melts at high temperature allows for the co-existence of a wide range of configurations and this would have important consequences for the compressional behavior of melts. Although our observations for the widths of some vibrational modes show that glasses can also have diverse configurations (Fig. 4), being a solid, it would be difficult for glasses to access as wide of a range of configurations as melts during compression due to kinetic effects at low temperature. In addition, previous experimental comparisons of glass and melt (Stebbins, 2008) found a first-order resemblance between the structures of glass and melt but differences in some properties at high temperature.

However, high-coordinated Si was found in alkali silicate glasses quenched from melts at high P–T, indicating that the Si coordination number increase does occur in melts at high pressure (Xue et al., 1989; Stebbins and McMillan, 1989; Xue et al., 1991). Moreover, alkali silicate glasses quenched from high P–T show compositional dependence on the population of high-coordinated Si (Xue et al., 1991), indicating

that the concentration of Si and ionic sizes of network modifiers are important factors for the structural transitions of silicate melts at high pressure similar to what we found on alkaline earth silicate glasses.

If the compositional dependence observed in $MgSiO_3$, Mg_2SiO_4, and $CaSiO_3$ glasses in this study occur in the corresponding melts at high *P–T*, it could influence differentiation in the early and present-day Earth's mantle. Dynamic and geochemical models support the existence of a deep magma ocean in the early Earth (Walter and Trønnes, 2004). At mid-depths in the magma ocean (20–40 GPa in the glasses), $MgSiO_3$ and Mg_2SiO_4 might be in different structural states over some depth range. In other words, Si-rich melt would be in a denser high-*P* structure, whereas Si-poor melt may still be in the low-*P* structure at this depth range. Consequently, Si-rich melts would have higher density and therefore become negatively buoyant compared to Si-poor melts at these transition depths, leading to compositional differentiation in the magma ocean. In crystalline phases, the ilmenite phase in $MgSiO_3$ and the spinel phase in Mg_2SiO_4 are stable over a similar depth range, yet all Si atoms are in 6-fold coordination in the ilmenite phase whereas they are in 4-fold coordination in the spinel phase. This structural difference results in 5% higher density in the ilmenite phase than the spinel phase.

This hypothesis requires processes for the separation of Si-rich and Si-poor melts. One possibility is some degree of compositional heterogeneity in the magma ocean. Another possibility is a liquid miscibility gap between $MgSiO_3$ and Mg_2SiO_4 at high pressure caused by the structural difference between the Si-rich and Si-poor melts. To our knowledge, no measurements have been performed for the MgO–SiO_2 system to sufficiently high *P* and *T*, in order to investigate this possibility.

It has long been debated whether the mantle is chemically stratified or whether a hidden geochemical reservoir exists in the mantle (Albarède and van der Hilst, 1999). Recently Boyet and Carlson (2005) showed that terrestrial samples have a higher $^{142}Nd/^{144}Nd$ ratio than chondrites, proposing a global chemical differentiation event in the young Earth ($\lesssim$30 Ma) that formed an enriched mantle reservoir hidden throughout the rest of Earth's history. However, the physical process responsible for the chemical differentiation is unknown. The compositional sensitivity for the structural transition in silicate melts might be an interesting possibility for the physical process.

Silicate melts may also play important roles in the differentiation of the present-day mantle, as there are lines of seismic evidence of melting atop the transition zone (Revenaugh and Sipkin, 1994; Song et al., 2004) and the CMB (Revenaugh and Meyer, 1997; Williams et al., 1998). Previous melting studies have shown that the eutectic composition shifts from near $MgSiO_3$ to Mg_2SiO_4 with pressure in the $MgSiO_3$–Mg_2SiO_4 system (Presnall et al., 1998; Zerr et al., 1998). If the compositional sensitivity of the structural transition we observed in Mg silicate glasses exists in the melts, near the transition zone, the possible appearance of a dense structure in Si-rich melts would help to gravitationally stabilize the melt. However, in the deep mantle, because the eutectic melting would produce an Si-poor composition the structural transition of which would be delayed, the structure alone may not stabilize the melts gravitationally and the role of Fe partitioning may be much more important.

This study demonstrates that Raman spectroscopy can capture important first-order features of the structural transition in the amorphous phases in MgO–SiO_2 at high pressure. Moreover, the transitions are sensitive to the composition of the glasses, consistent with studies on the alkali silicate glasses synthesized at high *P–T* (Xue et al., 1991). A pioneering vibrational spectroscopy work has been done for a silicate melt analog, $Na_2Ge_2O_5H_2O$, at in situ high *P–T* (Farber and Williams, 1992). However, direct measurements on Mg silicate melts still remain very challenging because of their extremely low scattering and the intense thermal radiation from the sample at high *T*. Recently, Raman scattering has been successfully measured at high temperature up to 2000 K using gated spectroscopy techniques (Goncharov and Crowhurst, 2005; Slotznick and Shim, 2008) and theoretically the measurements should be possible at even higher temperatures. Therefore, our glass results here would be an important guide for future vibrational spectroscopy studies on silicate melts at in situ high *P–T*. In addition, other synchrotron techniques are rapidly being improved for high-pressure studies of amorphous Mg silicates (Lee et al., 2008).

Acknowledgment

We thank J. Tangeman and R. Weber for the synthesis of glasses. Discussions with T. L. Grove, S. K. Lee, B. Grocholski, S. Speziale, and two anonymous reviewers improved the paper. N. Chatterjee assisted Electron Microprobe measurements. NSF supported the construction of Raman spectrometer (EAR-0337156) and the measurements of glasses (EAR-0337005). KC is supported by the DOE NNSA SSGF.

References

Agee, C.B., 1990. A new look at differentiation of the Earth from melting experiments on the Allende meteorite. Nature 346, 834–837.
Agee, C.B., Walker, D., 1988. Mass balance and phase density constraints on early differentiation of chondritic mantle. Earth Planet. Sci. Lett. 90, 144–156.
Akins, J.A., Luo, S.-N., Asimow, P.D., Ahrens, T.J., 2004. Shock-induced melting of $MgSiO_3$ perovskite and implications for melts in Earth's lowermost mantle. Geophys. Res. Lett. 31, L14612.
Albarède, F., van der Hilst, R.D., 1999. New mantle convection model may reconcile conflicting evidence. Eos Trans. 80, 535–539.
Boyet, M., Carlson, R.W., 2005. ^{142}Nd evidence for early (>4.53 Ga) global differentiation of the silicate earth. Science 309, 576–582.
Choquette, S.J., Etz, E.S., Hurst, W.S., Blackburn, D.H., Leigh, S.D., 2007. Relative intensity correction of Raman spectrometers: NIST SRMs 2241 through 2243 for 785 nm, 532 nm and 488 nm/514.4 nm excitation. Appl. Spectrosc. 61, 117–129.
Cooney, T.F., Sharma, S.K., 1990. Structure of glasses in the systems Mg_2SiO_4–Fe_2SiO_4, Mn_2SiO_4–Fe_2SiO_4, Mg_2SiO_4–$CaMgSiO_4$, and Mn_2SiO_4–$CaMnSiO_4$. J. Non-Cryst. Sol. 122, 10–32.
de Koker, N.P., Stixrude, L., Karki, B.B., 2008. Thermodynamics, structure, dynamics, and freezing of Mg_2SiO_4 liquid at high pressure. Geochim. Cosmochim. Acta 72, 1427–1441.
Durben, D.J., McMillan, P.F., Wolf, G.H., 1993. Raman study of the high-pressure behavior of forsterite (Mg_2SiO_4) crystal and glass. Am. Mineral. 78, 1143–1148.
Farber, D.L., Williams, Q., 1992. Pressure-induced coordination changes in alkali-germanate melts: an in situ spectroscopic investigation. Science 256, 1427–1430.
Gaudio, S.J., Sen, S., Lesher, C.E., 2008. Pressure-induced structural changes and densification of vitreous $MgSiO_3$. Geochim. Cosmochim. Acta 72, 1222–1230.
Goncharov, A.F., Crowhurst, J.C., 2005. Pulsed laser Raman spectroscopy in the laser-heated diamond anvil cell. Rev. Sci. Instrum. 76, 063905.
Hemley, R.J., Mao, H.K., Bell, P.M., Mysen, B.O., 1986. Raman spectroscopy of SiO_2 glasses at high pressure. Phys. Rev. Lett. 57, 747–750.
Ito, E., Takahashi, E., 1987. Melting of peridotite at uppermost lower-mantle conditions. Nature 328, 514–517.
Karki, B.B., Wentzcovitch, R.M., de Gironcoli, S., Baroni, S., 2000. Ab initio lattice dynamics of $MgSiO_3$ perovskite at high pressure. Phys. Rev. B 62, 14750–14756.
Kohara, S., Suzuya, K., Takeuchi, K., Loong, C.-K., Grimsditch, M., Weber, J.K.R., Tangeman, J.A., Key, T.S., 2004. Glass formation at the limit of insufficient network formers. Science 303, 1649–1652.
Kubicki, J.D., Hemley, R.J., Hofmeister, A.M., 1992. Raman and infrared study of pressure-induced structural changes in $MgSiO_3$, $CaMgSi_2O_6$, and $CaSiO_3$ glasses. Am. Mineral. 77, 258–269.
Lee, S.K., Fei, Y., Cody, G.D., Mysen, B.O., 2003. Order and disorder in sodium silicate glasses and melts at 10 GPa. Geophys. Res. Lett. 30, 1845.
Lee, S.K., Lin, J.-F., Cai, Y.Q., Hiraoka, N., Eng, P.J., Okuchi, T., Mao, H.-K., Meng, Y., Hu, M.Y., Chow, P., Shu, J., Li, B., Fukui, H., Lee, B.H., Kim, H.N., Yoo, C.-S., 2008. X-ray Raman scattering study of $MgSiO_3$ glass at high pressure: implication for triclustered $MgSiO_3$ melt in Earth's mantle. Proc. Natl. Acad. Sci. 105, 7925–7929.
Mackenzie, J.D., 1963a. High-pressure effects on oxide glasses: I. densification in rigid state. J. Am. Ceram. Soc. 46, 461–470.
Mackenzie, J.D., 1963b. High-pressure effects on oxide glasses: II. subsequent heat treatment. J. Am. Ceram. Soc. 46, 470–476.
Mao, H.-K., Xu, J., Bell, P.M., 1986. Calibration of the ruby pressure gauge to 800 kbar under quasihydrostatic conditions. J. Geophys. Res. 91, 4673–4676.
McMillan, P., 1984a. A Raman spectroscopic study of glasses in the system CaO–MgO–SiO_2. Am. Mineral. 69, 645–659.
McMillan, P., 1984b. Structural studies of silicate glasses and melts — applications and limitations of Raman spectroscopy. Am. Mineral. 69, 622–644.
McMillan, P., Piriou, B., Couty, R., 1984. A Raman study of pressure-densified vitreous silica. J. Chem. Phys. 81, 4234–4236.
Miller, G.H., Stolper, E.M., Ahrens, T.J., 1991. The equation of state of a molten komatiite. 2. Application to komatiite petrogenesis and the Hadean mantle. J. Geophys. Res. 96, 11849–11864.
Mookherjee, M., Stixrude, L., Karki, B., 2008. Hydrous silicate melt at high pressure. Nature 452, 983–986.

Mosenfelder, J.L., Asimow, P.D., Ahrens, T.J., 2007. Thermodynamic properties of Mg_2SiO_4 liquid at ultra-high pressures from shock measurements to 200 GPa on forsterite and wadsleyite. J. Geophys. Res. 112, B06208.
Murakami, M., Hirose, K., Kawamura, K., Sata, N., Ohishi, Y., 2004. Post-perovskite phase transition in $MgSiO_3$. Science 304, 855–858.
Navrotsky, A., 1980. Lower mantle phase transitions may generally have negative pressure–temperature slopes. Geophys. Res. Lett. 7, 709–711.
Ohtani, E., Kato, T., Sawamoto, H., 1986. Melting of a model chondritic mantle to 20 GPa. Nature 322, 352–353.
Piriou, B., McMillan, P., 1983. The high-frequency vibrational spectra of vitreous and crystalline orthosilicate. Am. Mineral. 68, 426–443.
Presnall, D.C., Weng, Y.-H., Milholland, C.S., Walter, M.J., 1998. Liquidus phase relations in the system MgO–$MgSiO_3$ at pressures up to 25 GPa — constraints on crystallization of a molten Hadean mantle. Phys. Earth Planet. Inter. 107, 83–95.
Revenaugh, J., Sipkin, S.A., 1994. Seismic evidence for silicate melt atop the 410-km mantle discontinuity. Nature 369, 474–476.
Revenaugh, J., Meyer, R., 1997. Seismic evidence of partial melt within a possibly ubiquitous low-velocity layer at the base of the mantle. Science 277, 670–673.
Rigden, S.M., Ahrens, T.J., Stolper, E.M., 1984. Densities of liquid silicates at high pressures. Science 226, 1071–1074.
Shen, G.Y., Rivers, M.L., Sutton, S.R., Sata, N., Prakapenka, V.B., Oxley, J., Suslick, K.S., 2004. The structure of amorphous iron at high pressures to 67 GPa measured in a diamond anvil cell. Phys. Earth Planet. Inter. 143–144, 481–495.
Shim, S.-H., Kubo, A., Duffy, T.S., 2007. Raman spectroscopy of perovskite and post-perovskite phases of $MgGeO_3$ to 123 GPa. Earth Planet. Sci. Lett. 260, 166–178.
Shim, S.-H., Catalli, K., Hustoft, J., Kubo, A., Prakapenka, V.B., Caldwell, W.A., Kunz, M., 2008. Crystal structure and thermoelastic properties of $(Mg_{0.91}Fe_{0.09})SiO_3$ postperovskite up to 135 GPa and 2700 K. Proc. Natl. Acad. Sci. 105, 7382–7386.
Slotznick, S.P., Shim, S.-H., 2008. In situ Raman spectroscopy measurements of $MgAl_2O_4$ spinel up to 1400 °C. Am. Mineral. 93, 470–476.
Song, T.-R.A., Helmberger, D.V., Grand, S.P., 2004. Low-velocity zone atop the 410-km seismic discontinuity in the northwestern United States. Nature 427, 530–533.
Stebbins, J.F., 2008. Temperature effects on the network structure of oxide melts and their consequences for configurational heat capacity. Chem. Geol. 256, 80–91.
Stebbins, J.F., McMillan, P., 1989. Five- and six-coordinated Si in $K_2Si_4O_9$ glass quenched from 1.9 GPa and 1200 °C. Am. Mineral. 74, 965–968.
Stixrude, L., Karki, B., 2005. Structure and freezing of $MgSiO_3$ liquid in Earth's lower mantle. Science 310, 297–299.
Stolper, E.M., Ahrens, T.J., 1987. On the nature of pressure-induced coordination changes in silicate melts and glasses. Geophys. Res. Lett. 14, 1231–1233.
Tangeman, J.A., Phillips, B.L., Navrotsky, A., Weber, J.K.R., Hixson, A.D., Key, T.S., 2001. Vitreous forsterite (Mg_2SiO_4): synthesis, structure, and thermochemistry. Geophys. Res. Lett. 28, 2517–2520.
Tonks, W.B., Melosh, H.J., 1993. Magma ocean formation due to giant impacts. J. Geophys. Res. 98, 5319–5333.
Walter, M.J., Trønnes, R.G., 2004. Early Earth differentiation. Earth Planet. Sci. Lett. 225, 253–269.
Wan, J.T.K., Duffy, T.S., Scandolo, S., Car, R., 2007. First-principles study of density, viscosity, and diffusion coefficients of liquid $MgSiO_3$ at condition of the Earth's deep mantle. J. Geophys. Res. 112, B03208.
Wentzcovitch, R.M., Stixrude, L., Karki, B.B., Kiefer, B., 2004. Akimotoite to perovskite phase transition in $MgSiO_3$. Geophys. Res. Lett. 31, L10611.
Wilding, M.C., Benmore, C.J., Tangeman, J.A., Sampath, S., 2004a. Coordination changes in magnesium silicate glasses. Europhys. Lett. 67, 212–218.
Wilding, M.C., Benmore, C.J., Tangeman, J.A., Sampath, S., 2004b. Evidence of different structures in magnesium silicate liquids: coordination changes in forsterite- to enstatite-composition glasses. Chem. Geol. 213, 281–291.
Williams, Q., Jeanloz, R., 1988. Spectroscopic evidence for pressure-induced coordination changes in silicate glasses and melts. Science 239, 902–906.
Williams, Q., McMillan, P., Cooney, T.F., 1989. Vibrational spectra of olivine composition glasses: the Mg–Mn join. Phys. Chem. Mineral. 16, 352–359.
Williams, Q., Revenaugh, J., Garnero, E., 1998. A correlation between ultra-low basal velocities in the mantle and hot spots. Science 280, 546–549.
Wolf, G.H., McMillan, P.F., 1995. Pressure effects on silicate melt structure and properties. In: Stebbins, J.F., P.F.M., D.B., Dingwell (Eds.), Structure, Dynamics and Properties of Silicate Melts. Reviews in Mineralogy, Vol. 32. Mineralogical Society of America.
Wolf, G.H., Durben, D.J., McMillan, P.F., 1990. High-pressure Raman spectroscopic study of sodium tetrasilicate ($Na_2Si_4O_9$) glass. J. Chem. Phys. 93, 2280–2288.
Xue, X., Stebbins, J.F., Kanzaki, M., Tronnes, R.G., 1989. Silicon coordination and speciation changes in a silicate liquid at high pressures. Science 245, 962–963.
Xue, X., Stebbins, J.F., Kanzaki, M., McMillan, P.F., Poe, B., 1991. Pressure-induced silicon coordination and tetrahedral structural changes in alkali oxide-silica melts up to 12 GPa: NMR, Raman, and infrared spectroscopy. Am. Mineral. 76, 8–26.
Yarger, J.L., Smith, K.H., Nieman, R.A., Diefenbacher, J., Wolf, G.H., Poe, B.T., McMillan, P.F., 1995. Al coordination changes in high-pressure aluminosilicate liquids. Science 270, 1964–1967.
Zerr, A., Diegeler, A., Boehler, R., 1998. Solidus of Earth's deep mantle. Science 281, 243–281.